

NCKU-HEP-98-14  
NCTU-HEP-9806

## Perturbative QCD study of the $B \rightarrow K^* \gamma$ decay

Hsiang-nan Li<sup>a</sup> and Guey-Lin Lin<sup>b</sup>

<sup>a</sup>Department of Physics, National Cheng-Kung University, Tainan 701, Taiwan, Republic of China

<sup>b</sup>Institute of Physics, National Chiao-Tung University, Hsinchu 300, Taiwan, Republic of China

### Abstract

We apply the perturbative QCD factorization theorem developed recently for nonleptonic heavy meson decays to the radiative decay  $B \rightarrow K^* \gamma$ . In this formalism the evolution of the Wilson coefficients from the  $W$  boson mass down to the characteristic scale of the decay process is governed by the effective weak Hamiltonian. The evolution from the characteristic scale to a lower hadronic scale is formulated by the Sudakov resummation. Besides computing the dominant contribution arising from the magnetic-penguin operator  $O_7$ , we also calculate the contributions of four-quark operators. By fitting our prediction for the branching ratio of the  $B \rightarrow K^* \gamma$  decay to the CLEO data, we determine the  $B$  meson wave function, that possesses a sharp peak at a low momentum fraction.

PACS numbers: 13.25.Hw, 11.10.Hi, 12.38.Bx

## I. INTRODUCTION

The observation of the decay  $B \rightarrow K^* \gamma$  five years ago [1] opened a new era for particle physics, since the penguin structure of the electroweak theory was probed for the first time. Soon after this observation, the inclusive  $B \rightarrow X_s \gamma$  decay [2] was also established. The updated branching ratios for both decays are  $(4.2 \pm 0.8 \pm 0.6) \times 10^{-5}$  [3] and  $(3.14 \pm 0.48) \times 10^{-4}$  [4,5], respectively. In recent literatures, the inclusive decay  $B \rightarrow X_s \gamma$  receives more attentions than the exclusive mode  $B \rightarrow K^* \gamma$ . The branching ratio and the photon energy spectrum of the  $B \rightarrow X_s \gamma$  decay have been used to constrain the parameter-space of the new physics beyond the standard model. The preference of studying the inclusive mode is clear in that its hadronic dynamics is much easier to handle as compared to the exclusive mode. It has been shown that, to the leading order in  $1/M_b$ ,  $M_b$  being the  $b$  quark mass, the branching ratio  $\mathcal{B}(B \rightarrow X_s \gamma)$  is given by the branching ratio  $\mathcal{B}(b \rightarrow s \gamma)$  of the corresponding quark-level process. Furthermore, the sub-leading  $1/M_b$ -corrections can be parametrized systematically using the heavy quark effective theory [6].

The hadronic dynamics of the exclusive decay  $B \rightarrow K^* \gamma$  is much more complicated. Specifically, one has to deal with the soft dynamics involved in the  $B$  and  $K^*$  mesons. Since the final states are light compared to the decaying  $B$  meson, one anticipates that perturbative QCD (PQCD) is applicable to this process because of the large energy release. In fact, the PQCD formalism based upon factorization theorems, which incorporates the Sudakov resummation of soft-gluon effects, has been developed for sometime [7–9], and applied to semileptonic [7,8], inclusive-radiative [9] and nonleptonic  $B$  meson decays [10]. This approach is so far rather successful. In this article, we shall extend this formalism to penguin-induced exclusive processes, such as the  $B \rightarrow K^* \gamma$  decay. The satisfactory result with respect to this complicated process, as presented later, provides further confidence on the validity of the PQCD approach to  $B$  meson decays.

According to the PQCD factorization theorem, the branching ratio of a heavy meson decay is expressed as the convolution of a hard subamplitude with meson wave functions. The former, with at least one hard gluon attaching to the spectator quark, is calculable in the usual perturbation theory, while the latter must be extracted from the experimental data or derived by nonperturbative methods, such as QCD sum rules. Since the  $K^*$  meson wave function has been known from the sum rule analyses [11,12], the  $B \rightarrow K^* \gamma$  decay is an ideal process from which the unknown  $B$  meson wave function can be determined. With the  $B$  meson wave function obtained here, we are able to make predictions for other  $B$  meson decay modes, especially for the charmless decays. We shall show that by fitting our prediction for the branching ratio  $\mathcal{B}(B \rightarrow K^* \gamma)$  to the CLEO data, a  $B$  meson wave function with a sharp peak at the low momentum fraction is obtained.

Comparing our work to others, we remark that most of the previous studies on this decay focus only on the contribution of the magnetic-penguin operator  $O_7$ , and their approaches are based upon quark models. To ensure that other contributions are indeed negligible, we also calculate the contribution by the current-current operator  $O_2$ , which arises through the four-point  $b \rightarrow sg^* \gamma$  coupling with the off-shell gluon reabsorbed by a spectator quark. Although such a contribution has been calculated before [13], it is however obtained in a naive PQCD framework which does not include the Sudakov resummation and the renormalization-group (RG) analysis [13]. As a result, the predictions of Ref. [13] are sensitive to the choice of

the renormalization scale  $\mu$ . In our more completed approach, the sensitivity to  $\mu$  can be avoided. We find that, due to certain cancellations, the contribution by  $O_2$  turns out to be rather small.

We also like to comment on a different viewpoint based on the overlap integral of meson wave functions [14], which showed that the diagrams without any hard gluon dominate over those we will be considering here. We shall argue that the observation in [14] is due to an underestimation on the value of the strong coupling constant and a choice of a flat  $B$  meson wave function. If evaluating the coupling constant at the characteristic momentum flow involved in the decay process [13], and employing a sharper  $B$  meson wave function, these higher-order contributions may become comparable to the leading-order ones. Hence, the approach in [14] does not seem to be self-consistent. In our approach, the diagrams without hard gluons do not contribute under our parametrization of parton momenta. Therefore, the diagrams with a hard gluon attaching to a spectator are leading in our analysis.

This article is organized as follows: In Sect. II, we write down the effective Hamiltonian for the  $B \rightarrow K^*\gamma$  decay. In particular, the current-current operator  $O_2$  and the magnetic-penguin operators  $O_7$  are identified as major sources of the contribution. We then calculate the  $O_2$ -induced  $b \rightarrow sg^*\gamma$  vertex, keeping the gluon line off-shell. In Sect. III, we derive the factorization formulas for the  $B \rightarrow K^*\gamma$  decay, which include contributions from the various operators. The numerical result is presented in Sect. IV, where the contribution of each operator is compared. Sect. V is the conclusion.

## II. EFFECTIVE HAMILTONIAN

The effective Hamiltonian for the flavor-changing  $b \rightarrow s$  transition is now standard, which is given by [15,16]

$$H_{\text{eff}}(b \rightarrow s\gamma) = -\frac{G_F}{\sqrt{2}} V_{ts}^* V_{tb} \sum_{i=1}^8 C_i(\mu) O_i(\mu) \quad (1)$$

with

$$\begin{aligned} O_1 &= (\bar{s}_i c_j)_{V-A} (\bar{c}_j b_i)_{V-A} \\ O_2 &= (\bar{s}_i c_i)_{V-A} (\bar{c}_j b_j)_{V-A} \\ O_3 &= (\bar{s}_i b_i)_{V-A} \sum_q (\bar{q}_j q_j)_{V-A} \\ O_4 &= (\bar{s}_i b_j)_{V-A} \sum_q (\bar{q}_j q_i)_{V-A} \\ O_5 &= (\bar{s}_i b_i)_{V-A} \sum_q (\bar{q}_j q_j)_{V+A} \\ O_6 &= (\bar{s}_i b_j)_{V-A} \sum_q (\bar{q}_j q_i)_{V+A} \\ O_7 &= \frac{e}{4\pi^2} \bar{s}_i \sigma^{\mu\nu} (m_s P_L + m_b P_R) b_i F_{\mu\nu} \\ O_8 &= \frac{g}{4\pi^2} \bar{s}_i \sigma^{\mu\nu} (m_s P_L + m_b P_R) T_{ij}^a b_j G_{\mu\nu}^a, \end{aligned} \quad (2)$$

$i, j$  being the color indices. In the PQCD picture, the lowest-order diagrams for the  $B \rightarrow K^*\gamma$  decay arising from operators  $O_2$ ,  $O_7$  and  $O_8$  are depicted in Figs. 1-3. It is not hard to see that contributions other than the above are negligible. For example, contributions depicted in Fig. 4 are very suppressed, although they are of the same order,  $O(eG_F\alpha_s)$  [17], as those of Figs. 1-3. We draw this conclusion from a previous experience with  $B \rightarrow D^*\gamma$ . Indeed, from a diagram similar to Fig. 4 (with  $s$  replaced by  $c$ , and the  $\bar{q}$  on both sides replaced by  $\bar{d}$  and  $\bar{u}$ , respectively), one has obtained  $\mathcal{B}(B \rightarrow D^*\gamma) = 10^{-6}$  [18]. Since  $f_{K^*} \approx f_{D^*}$ , and  $V_{tb}V_{ts}$  is comparable to  $V_{cb}V_{ud}$ , it is clear that the diagram in Fig. 4 gives  $\mathcal{B}(B \rightarrow K^*\gamma) \approx 10^{-6} \times C_{3(4,5,6)}^2 \approx 10^{-9} - 10^{-10}$ , and is thus negligible. There is still one more type of contributions of the same order as shown in Fig. 5. By an explicit calculation, one can show that such contributions merely give corrections to the Wilson coefficients  $C_3$ - $C_6$  occurring in Fig. 4. Hence, they are negligible as well. Finally, in Sect. IV, we shall see that the contribution by  $O_8$  is also negligible.

Before implementing the PQCD formalism to evaluate the contributions of Figs. 1-3, we compute the four-point  $b \rightarrow sg^*\gamma$  vertex. The on-shell  $b \rightarrow sg\gamma$  vertex has been calculated in [19] sometime ago. Here we generalize the result to the case with an off-shell gluon [20]. We first perform a Fierz transformation on  $O_2$ , *i.e.*,

$$O_2 \equiv (\bar{s}_i c_i)_{V-A} (\bar{c}_j b_j)_{V-A} = (\bar{s}_i b_j)_{V-A} (\bar{c}_j c_i)_{V-A}. \quad (3)$$

The  $b(p) \rightarrow s(p')\gamma(k_1)g^*(k_2)$  vertex is expressed as

$$I^{\mu\nu} = C_2 V_{ts}^* V_{tb} \bar{u}(p') \frac{1}{2} \gamma^\rho (1 - \gamma_5) T^a u(p) I_{\mu\nu\rho} \epsilon^\mu(k_1), \quad (4)$$

with the structure-tensor

$$\begin{aligned} I_{\mu\nu\rho} = & A_1 \epsilon_{\mu\nu\rho\sigma} k_1^\sigma + A_2 \epsilon_{\mu\nu\rho\sigma} k_2^\sigma + A_3 \epsilon_{\mu\rho\sigma\tau} k_1^\sigma k_2^\tau k_{1\nu} \\ & + A_4 \epsilon_{\nu\rho\sigma\tau} k_1^\sigma k_2^\tau k_{2\mu} + A_5 \epsilon_{\mu\rho\sigma\tau} k_1^\sigma k_2^\tau k_{2\nu} + A_6 \epsilon_{\nu\rho\sigma\tau} k_1^\sigma k_2^\tau k_{1\mu}. \end{aligned} \quad (5)$$

Clearly, the form factor  $A_6$  can be discarded because of  $k_1 \cdot \epsilon(k_1) = 0$ . From the requirement of gauge invariance, *i.e.*,  $k_1^\mu I_{\mu\nu\rho} = 0$  and  $k_2^\nu I_{\mu\nu\rho} = 0$ , we have

$$\begin{aligned} A_2 + A_4 k_1 \cdot k_2 &= 0 \\ A_1 + A_3 k_1 \cdot k_2 + A_5 k_2^2 &= 0. \end{aligned} \quad (6)$$

The invariance of  $I_{\mu\nu\rho}$  under the interchanges  $k_1 \leftrightarrow k_2$  and  $\mu \leftrightarrow \nu$  further require  $A_3 = -A_4$ . With the above relations,  $I_{\mu\nu\rho}$  is simplified into

$$\begin{aligned} I_{\mu\nu\rho} = & A_4 [k_1 \cdot k_2 \epsilon_{\mu\nu\rho\sigma} (k_1 - k_2)^\sigma + \epsilon_{\nu\rho\sigma\tau} k_1^\sigma k_2^\tau k_{2\mu} - \epsilon_{\mu\rho\sigma\tau} k_1^\sigma k_2^\tau k_{1\nu}] \\ & + A_5 (\epsilon_{\mu\rho\sigma\tau} k_1^\sigma k_2^\tau k_{2\nu} - k_2^2 \epsilon_{\mu\nu\rho\sigma} k_1^\sigma), \end{aligned} \quad (7)$$

with

$$A_4 = \frac{2\sqrt{2}}{3\pi^2} e g_s G_F I_{11}(M_c^2), \quad (8)$$

$$A_5 = -\frac{2\sqrt{2}}{3\pi^2} e g_s G_F [I_{10}(M_c^2) - I_{20}(M_c^2)], \quad (9)$$

and

$$I_{ab}(m^2) = \int_0^1 dx \int_0^{1-x} dy \frac{x^a y^b}{x(1-x)k_2^2 + 2xyk_1 \cdot k_2 - m^2 + i\varepsilon}. \quad (10)$$

Carrying out the Feynman-parameter integrations, we obtain

$$I_{11}(m^2) = \left[ \frac{1}{2Q^2} + \int_0^1 dx \frac{m^2 - x(1-x)k_2^2}{xQ^4} \ln \left| \frac{m^2 - x(1-x)(k_2^2 + Q^2)}{m^2 - x(1-x)k_2^2} \right| - i\pi\Theta(Q^2 + k_2^2 - 4m^2) \left( \frac{m^2}{Q^4} \ln \frac{1+\beta}{1-\beta} - \frac{\beta k_2^2}{2Q^4} \right) \right], \quad (11)$$

$$I_{10}(m^2) - I_{20}(m^2) = \left[ \int_0^1 dx \frac{1-x}{Q^2} \ln \left| \frac{m^2 - x(1-x)(k_2^2 + Q^2)}{m^2 - x(1-x)k_2^2} \right| - i\pi\Theta(Q^2 + k_2^2 - 4m^2) \frac{\beta}{2Q^2} \right], \quad (12)$$

with  $Q^2 = 2k_1 \cdot k_2$ , and  $\beta = \sqrt{1 - 4m^2/(k_2^2 + Q^2)}$ . As a side remark, we note that both  $I_{11}(m^2)$  and  $I_{10}(m^2) - I_{20}(m^2)$  have smooth limits as  $m^2 \rightarrow 0$ . Hence, we can safely neglect the contributions of  $O_4$  and  $O_6$  to the  $b \rightarrow sg^*\gamma$  vertex, since their Wilson coefficients,  $C_4$  and  $C_6$ , are much smaller than  $C_2$ .

Having determined the  $b \rightarrow sg^*\gamma$  vertex, we attach the off-shell gluon line to the spectator quark to form the  $B \rightarrow K^*\gamma$  amplitude as shown in Fig. 1. As mentioned, this amplitude is of the order  $e\alpha_s G_F$ , the same as the amplitudes induced by  $O_7$  and  $O_8$  depicted in Figs. 2 and 3, respectively. In the next section, we shall compute the contribution of each operator to the  $B \rightarrow K^*\gamma$  decay using the PQCD factorization theorem.

### III. FACTORIZATION FORMULAS

In this section we first review the PQCD factorization theorem developed for nonleptonic heavy meson decays [10], and then extend it to the  $B \rightarrow K^*\gamma$  decay. Nonleptonic heavy meson decays involve three scales: the  $W$  boson mass  $M_W$ , at which the matching conditions of the effective Hamiltonian to the original Hamiltonian are defined, the typical scale  $t$  of a hard subamplitude, which reflects the dynamics of heavy meson decays, and the factorization scale  $1/b$ , with  $b$  the conjugate variable of parton transverse momenta. The dynamics below  $1/b$  is regarded as being completely nonperturbative, and parametrized into a meson wave function  $\phi(x)$ ,  $x$  being the momentum fraction. Above the scale  $1/b$ , PQCD is reliable and radiative corrections produce two types of large logarithms:  $\ln(M_W/t)$  and  $\ln(tb)$ . The former are summed by RG equations to give the evolution from  $M_W$  down to  $t$  described by the Wilson coefficients  $c(t)$ . While the latter are summed to give the evolution from  $t$  to  $1/b$ .

There exist also double logarithms  $\ln^2(Pb)$  from the overlap of collinear and soft divergences,  $P$  being the dominant light-cone component of a meson momentum. The resummation of these double logarithms leads to a Sudakov form factor  $\exp[-s(P, b)]$ , which suppresses the long-distance contributions in the large  $b$  region, and vanishes as  $b = 1/\Lambda$ ,  $\Lambda \equiv \Lambda_{\text{QCD}}$  being the QCD scale. This factor improves the applicability of PQCD around

the energy scale of few GeV. The  $b$  quark mass scale is located in the range of applicability. This is the motivation we develop the PQCD formalism for heavy hadron decays. For the detailed derivation of the relevant Sudakov form factors, please refer to [7,8].

With all the large logarithms organized, the remaining finite contributions are absorbed into a hard  $b$  quark decay subamplitude  $H(t)$ . Because of Sudakov suppression, the perturbative expansion of  $H$  in the coupling constant  $\alpha_s$  makes sense. Therefore, a three-scale factorization formula is given by the typical expression,

$$c(t) \otimes H(t) \otimes \phi(x) \otimes \exp \left[ -s(P, b) - 2 \int_{1/b}^t \frac{d\bar{\mu}}{\bar{\mu}} \gamma_q(\alpha_s(\bar{\mu})) \right], \quad (13)$$

where the exponential containing the quark anomalous dimension  $\gamma_q = -\alpha_s/\pi$  describes the evolution from  $t$  to  $1/b$  mentioned above. The explicit expression of the exponent  $s$  can be found in [10]. Since logarithmic corrections have been summed by RG equations, the above factorization formula does not depend on the renormalization scale  $\mu$  [10]. Our formalism then avoids the sensitivity to  $\mu$  that appears in [13].

We now apply the three-scale factorization theorem to the radiative decay  $B \rightarrow K^* \gamma$ , whose effective Hamiltonian has been given in the previous section. As stated before, only the operators  $O_2$ ,  $O_7$  and  $O_8$  are crucial, to which the corresponding diagrams and hard subamplitudes are shown in Figs. 1-3 and Table I, respectively. We write the momenta of  $B$  and  $K^*$  mesons in light-cone coordinates as  $P_B = (M_B/\sqrt{2})(1, 1, \mathbf{0}_T)$  and  $P_K = (M_B/\sqrt{2})(1, r^2, \mathbf{0}_T)$ , respectively, with  $r = M_{K^*}/M_B$ . The  $B$  meson is at rest with the above choice of momenta. We further parametrize the momenta of the light valence quarks in the  $B$  and  $K^*$  mesons as  $k_B$  and  $k_K$ , respectively.  $k_B$  has a minus component  $k_B^-$ , giving the momentum fraction  $x_B = k_B^-/P_B^-$ , and small transverse components  $\mathbf{k}_{BT}$ .  $k_K$  has a large plus component  $k_K^+$ , giving  $x_K = k_K^+/P_K^+$ , and small  $\mathbf{k}_{KT}$ . The photon momentum is then  $P_\gamma = P_B - P_K$ , whose nonvanishing component is only  $P_\gamma^-$ .

The  $B \rightarrow K^* \gamma$  decay amplitude can be decomposed as

$$M = \epsilon_\gamma^* \cdot \epsilon_{K^*}^* M^S + i \epsilon_{\mu\rho+-} \epsilon_\gamma^{*\mu} \epsilon_{K^*}^{*\rho} M^P, \quad (14)$$

with  $\epsilon_\gamma$  and  $\epsilon_{K^*}$  the polarization vectors of the photon and of the  $K^*$  meson, respectively. Note that we have neglected the structure  $(P_\gamma \cdot \epsilon_{K^*}^*)(P_K \cdot \epsilon_\gamma^*)/(P_\gamma \cdot P_K)$  which should come together with  $\epsilon_\gamma^* \cdot \epsilon_{K^*}^*$ . This is due to our choice of the frame which gives  $P_K \cdot \epsilon_\gamma^* = 0$ . From Eq. (14), it is obvious that only the  $K^*$  mesons with transverse polarizations are produced in the decay.

The total rate of the  $B \rightarrow K^* \gamma$  decay is given by

$$\Gamma = \frac{1-r^2}{8\pi M_B} (|M^S|^2 + |M^P|^2). \quad (15)$$

We can further decompose  $M^S$  and  $M^P$  as

$$M^i = M_2^i + M_7^i + M_8^i, \quad (16)$$

where  $i = S$  or  $P$ , and the terms on the right-hand side represent contributions from operators  $O_2$ ,  $O_7$ , and  $O_8$ , respectively.

In the following, we write the factorization formulas for  $M_l^i$  in terms of the overall factor

$$\Gamma^{(0)} = \frac{G_F}{\sqrt{2}} \frac{e}{\pi} V_{ts}^* V_{tb} C_F M_B^5 . \quad (17)$$

The amplitudes contributed by  $O_2$  is written as

$$\begin{aligned} M_2^S &= \Gamma^{(0)} \frac{4}{3} \int_0^1 dx \int_0^{1-x} dy \int_0^1 dx_B dx_K \int_0^{1/\Lambda} bdb \phi_B(x_B) \phi_{K^*}(x_K) \\ &\quad \times \alpha_s(t_2) c_2(t_2) \exp[-S(x_B, x_K, t_2, b, b)] \\ &\quad \times [(1-r^2 + 2rx_K + 2x_B)y - (rx_K + 3x_B)(1-x)] \\ &\quad \times \frac{(1-r)(1-r^2)x_K x}{xy(1-r^2)x_K M_B^2 - M_c^2} H_2(Ab, \sqrt{|B_2^2|}b) , \end{aligned} \quad (18)$$

$$\begin{aligned} M_2^P &= \Gamma^{(0)} \frac{4}{3} \int_0^1 dx \int_0^{1-x} dy \int_0^1 dx_B dx_K \int_0^{1/\Lambda} bdb \phi_B(x_B) \phi_{K^*}(x_K) \\ &\quad \times \alpha_s(t_2) c_2(t_2) \exp[-S(x_B, x_K, t_2, b, b)] \\ &\quad \times \left[ \left( (1-r)(1-r^2) + 2r^2 x_K + 2x_B \right) y \right. \\ &\quad \left. - (r(1+r)x_K + (3-r)x_B)(1-x) \right] \\ &\quad \times \frac{(1-r^2)x_K x}{xy(1-r^2)x_K M_B^2 - M_c^2} H_2(Ab, \sqrt{|B_2^2|}b) , \end{aligned} \quad (19)$$

with

$$\begin{aligned} A^2 &= x_K x_B M_B^2 , \\ B_2^2 &= x_K x_B M_B^2 - \frac{y}{1-x} (1-r^2) x_K M_B^2 + \frac{M_c^2}{x(1-x)} , \\ t_2 &= \max(A, \sqrt{|B_2^2|}, 1/b) . \end{aligned} \quad (20)$$

To arrive at the above expressions, we have employed Eq. (10) for the charm loop integral, instead of Eqs. (11) and (12). The variable  $b_B$  ( $b_K$ ), conjugate to the parton transverse momentum  $k_{BT}$  ( $k_{KT}$ ), represents the transverse extent of the  $B$  ( $K^*$ ) meson;  $t_2$  is the characteristic scale of the hard subamplitude

$$\begin{aligned} H_2(Ab, \sqrt{|B_2^2|}b) &= K_0(Ab) - K_0(\sqrt{|B_2^2|}b) , \quad B_2^2 > 0 , \\ &= K_0(Ab) - i \frac{\pi}{2} H_0^{(1)}(\sqrt{|B_2^2|}b) , \quad B_2^2 < 0 , \end{aligned} \quad (21)$$

which comes from the Fourier transform of the corresponding expressions in Table I to the  $b$  space. Note that, for simplicity in the notation, we have used  $H_2$  to denote hard subamplitudes in both  $M_2^S$  and  $M_2^P$ . In Table I, these two amplitudes are distinguished.

There are two diagrams, Figs. 2(a) and 2(b), associated with the operator  $O_7$ , where the hard gluon connects both quarks of the  $B$  meson or those of the  $K^*$  meson. The amplitudes from the two diagrams are

$$\begin{aligned}
M_7^S = -M_7^P &= \Gamma^{(0)} 2 \int_0^1 dx_B dx_K \int_0^{1/\Lambda} b_B db_B b_K db_K \phi_B(x_B) \phi_{K^*}(x_K) (1 - r^2) \\
&\times \left[ r H_7^{(a)}(Ab_K, \sqrt{|B_7^2|} b_B, \sqrt{|B_7^2|} b_K) F_7(t_{7a}) \right. \\
&\left. + [1 + r + (1 - 2r)x_K] H_7^{(b)}(Ab_B, C_7 b_B, C_7 b_K) F_7(t_{7b}) \right], \quad (22)
\end{aligned}$$

with

$$\begin{aligned}
B_7^2 &= (x_B - r^2) M_B^2, \quad C_7^2 = x_K M_B^2 \\
t_{7a} &= \max(A, \sqrt{|B_7^2|}, 1/b_B, 1/b_K), \\
t_{7b} &= \max(A, C_7, 1/b_B, 1/b_K), \quad (23)
\end{aligned}$$

where the function  $F_7$  denotes the product

$$F_7(t) = \alpha_s(t) c_7(t) \exp[-S(x_B, x_K, t, b_B, b_K)]. \quad (24)$$

The hard functions

$$\begin{aligned}
H_7^{(a)}(Ab_K, \sqrt{|B_7^2|} b_B, \sqrt{|B_7^2|} b_K) &= \\
K_0(Ab_K) h(\sqrt{|B_7^2|} b_B, \sqrt{|B_7^2|} b_K), \quad B_7^2 > 0, \\
K_0(Ab_K) h'(\sqrt{|B_7^2|} b_B, \sqrt{|B_7^2|} b_K), \quad B_7^2 < 0, \quad (25)
\end{aligned}$$

with

$$\begin{aligned}
h &= \theta(b_B - b_K) K_0(\sqrt{|B_7^2|} b_B) I_0(\sqrt{|B_7^2|} b_K) + (b_B \leftrightarrow b_K), \\
h' &= i \frac{\pi}{2} \left[ \theta(b_B - b_K) H_0^{(1)}(\sqrt{|B_7^2|} b_B) J_0(\sqrt{|B_7^2|} b_K) + (b_B \leftrightarrow b_K) \right], \quad (26)
\end{aligned}$$

and

$$H_7^{(b)}(Ab_B, C_7 b_B, C_7 b_K) = K_0(Ab_B) h(C_7 b_B, C_7 b_K), \quad (27)$$

are derived from Figs. 2(a) and 2(b), respectively. The relation  $M_7^S = -M_7^P$  reflects the equality of the parity-conserving and parity-violating contributions induced by  $O_7$ .

Four diagrams, Figs. 3(a)-(d), are associated with the operator  $O_8$ , where the photon is radiated by each quark in the  $B$  or  $K^*$  mesons. The corresponding amplitudes are

$$\begin{aligned}
M_8^S &= -\Gamma^{(0)} \frac{1}{3} \int_0^1 dx_B dx_K \int_0^{1/\Lambda} b_B db_B b_K db_K \phi_B(x_B) \phi_{K^*}(x_K) \\
&\times \left\{ (1 - r^2 + x_B)(rx_K + x_B) H_8^{(a)}(Ab_K, B_8 b_B, B_8 b_K) F_8(t_{8a}) \right. \\
&+ [(2 - 3r)x_K - x_B + r(1 - x_K)(rx_K - 2rx_B + 3x_B)] \\
&\quad \times H_8^{(b)}(Ab_B, C_8 b_B, C_8 b_K) F_8(t_{8b}) \\
&+ (1 + r)(1 - r^2)[(1 + r)x_B - rx_K] \\
&\quad \times H_8^{(c)}(\sqrt{|A'^2|} b_K, D_8 b_B, D_8 b_K) F_8(t_{8c}) \left. \right\}
\end{aligned}$$

$$\begin{aligned}
& -[(1-r^2)((1-r^2)(2-x_K)+(1+3r)(2x_K-x_B)) \\
& \quad +2r^2x_K(x_K-x_B)] \\
& \quad \times H_8^{(d)}(\sqrt{|A'^2|}b_B, E_8b_B, E_8b_K)F_8(t_{8d}) \Big\} , \tag{28}
\end{aligned}$$

$$\begin{aligned}
M_8^P = & \Gamma^{(0)} \frac{1}{3} \int_0^1 dx_B dx_K \int_0^{1/\Lambda} b_B db_B b_K db_K \phi_B(x_B) \phi_{K^*}(x_K) \\
& \times \left\{ (1-r^2+x_B)(rx_K+x_B) H_8^{(a)}(Ab_K, B_8b_B, B_8b_K)F_8(t_{8a}) \right. \\
& \quad + [(2-3r)x_K-x_B-r(1-x_K)(rx_K-2rx_B+3x_B)] \\
& \quad \times H_8^{(b)}(Ab_B, C_8b_B, C_8b_K)F_8(t_{8b}) \\
& \quad + (1-r)(1-r^2)[(1+r)x_B-rx_K] \\
& \quad \times H_8^{(c)}(\sqrt{|A'^2|}b_K, D_8b_B, D_8b_K)F(t_{8c}) \\
& \quad - [(1-r^2)((1-r^2)(2+x_K)-(1-3r)x_B) \\
& \quad - 2r^2x_K(x_K-x_B)] \\
& \quad \times H_8^{(d)}(\sqrt{|A'^2|}b_B, E_8b_B, E_8b_K)F(t_{8d}) \Big\} , \tag{29}
\end{aligned}$$

with

$$\begin{aligned}
A'^2 &= (1-r^2)(x_B-x_K)M_B^2 , \quad B_8^2 = (1-r^2+x_B)M_B^2 , \\
C_8^2 &= (1-x_K)M_B^2 , \quad D_8^2 = (1-r^2)x_BM_B^2 , \quad E_8^2 = (1-r^2)x_KM_B^2 , \\
t_{8a} &= \max(A, B_8, 1/b_B, 1/b_K) , \\
t_{8b} &= \max(A, C_8, 1/b_B, 1/b_K) , \\
t_{8c} &= \max(\sqrt{|A'^2|}, D_8, 1/b_B, 1/b_K) , \\
t_{8d} &= \max(\sqrt{|A'^2|}, E_8, 1/b_B, 1/b_K) . \tag{30}
\end{aligned}$$

and the function  $F_8$ ,

$$F_8(t) = \alpha_s(t)c_8(t) \exp[-S(x_B, x_K, t, b_B, b_K)] . \tag{31}$$

The hard functions

$$\begin{aligned}
H_8^{(a)}(Ab_K, B_8b_B, B_8b_K) &= H_7^{(b)}(Ab_K, B_8b_B, B_8b_K) , \\
H_8^{(b)}(Ab_B, C_8b_B, C_8b_K) &= K_0(Ab_B)h'(C_8b_B, C_8b_K) \\
H_8^{(c)}(\sqrt{|A'^2|}b_K, D_8b_B, D_8b_K) &= \\
& K_0(\sqrt{|A'^2|}b_K)h(D_8b_B, D_8b_K) , \quad A'^2 \geq 0 , \\
& i\frac{\pi}{2}H_0^{(1)}(\sqrt{|A'^2|}b_K)h(D_8b_B, D_8b_K) , \quad A'^2 < 0 , \\
H_8^{(d)}(\sqrt{|A'^2|}b_B, E_8b_B, E_8b_K) &= \\
& K_0(\sqrt{|A'^2|}b_B)h'(E_8b_B, E_8b_K) , \quad A'^2 \geq 0 , \\
& i\frac{\pi}{2}H_0^{(1)}(\sqrt{|A'^2|}b_B)h'(E_8b_B, E_8b_K) , \quad A'^2 < 0 \tag{32}
\end{aligned}$$

are derived from Figs. 3(a)-(d), respectively. It is obvious that the above factorization formulas bear the features of Eq. (13).

The exponentials  $\exp(-S)$  appearing in  $M_l^i$  are the complete Sudakov form factors with the exponent

$$S = s(x_B P_B^-, b_B) + 2 \int_{1/b_B}^t \frac{d\mu}{\mu} \gamma_q(\alpha_s(\mu)) + s(x_K P_K^+, b_K) + s((1-x_K) P_K^+, b_K) + 2 \int_{1/b_K}^t \frac{d\mu}{\mu} \gamma_q(\alpha_s(\mu)). \quad (33)$$

The wave functions  $\phi_B$  and  $\phi_{K^*}$  satisfy the normalization,

$$\int_0^1 \phi_i(x) dx = \frac{f_i}{2\sqrt{6}}, \quad (34)$$

with the decay constant  $f_i$ ,  $i = B$  and  $K^*$ . The wave function for the  $K^*$  meson with transverse polarizations has been derived using QCD sum rules [12], which is given by

$$\phi_{K^*} = \frac{f_{K^*}}{\sqrt{6}} \frac{15}{4} (1 - \xi^2) * [0.267(1 - \xi^2)^2 + 0.017 + 0.21\xi^3 + 0.07\xi], \quad (35)$$

with  $\xi = 1 - 2x$ . As to the  $B$  meson wave functions, we employ two models [21,22],

$$\phi_B^{(I)}(x) = \frac{N_B x(1-x)^2}{M_B^2 + C_B(1-x)}, \quad (36)$$

$$\phi_B^{(II)}(x) = N'_B \sqrt{x(1-x)} \exp \left[ -\frac{1}{2} \left( \frac{xM_B}{\omega} \right)^2 \right], \quad (37)$$

where  $N_B$  and  $N'_B$  are normalization constants; while  $C_B$  and  $\omega$  are shape parameters.

#### IV. RESULTS AND DISCUSSIONS

In the evaluation of the various form factors and amplitudes, we adopt  $G_F = 1.16639 \times 10^{-5}$  GeV $^{-2}$ , the flavor number  $n_f = 5$ , the decay constants  $f_B = 200$  MeV and  $f_{K^*} = 220$  MeV, the CKM matrix elements  $|V_{ts}^* V_{tb}| = 0.04$ , the masses  $M_c = 1.5$  GeV,  $M_B = 5.28$  GeV and  $M_{K^*} = 0.892$  GeV, the  $\bar{B}^0$  meson lifetime  $\tau_{B^0} = 1.53$  ps, and the QCD scale  $\Lambda = 0.2$  GeV [10]. We find that, no matter what value of the shape parameter  $C_B$  is chosen, the model  $\phi_B^{(I)}$  in Eq. (36) with a flat profile leads to results smaller than the CLEO data which gives  $\mathcal{B}(B \rightarrow K^* \gamma) = (4.2 \pm 0.8 \pm 0.6) \times 10^{-5}$  [3]. In fact, the maximal prediction from  $\phi_B^{(I)}$ , corresponding to the shape parameter  $C_B = -M_B^2$ , is about  $3.0 \times 10^{-5}$ , close to the lower bound of the data.

On the other hand, using model  $\phi_B^{(II)}$  in Eq. (37) with a sharp peak at small  $x$ , we obtain a prediction much closer to the experimental data. It is indeed found that, as  $\omega = 0.795$  GeV, a prediction  $4.204 \times 10^{-5}$  for the branching ratio is reached, which is equal to the central value of the experimental data. If varying the shape parameter to both  $\omega = 0.79$  GeV and  $\omega = 0.80$  GeV, we obtain the branching ratios  $4.25 \times 10^{-5}$  and  $4.14 \times 10^{-5}$ , respectively. It indicates that the allowed range for  $\omega$  is wide due to the yet large uncertainties of the data.

The detailed contribution from each amplitude  $M_l^i$  is listed in Table II in the unit of  $10^{-6}$  GeV $^{-2}$ . It is clear that  $M_7^S$  and  $M_7^P$  together give dominant contributions to the decay width. One also sees that  $M_2^S$  and  $M_2^P$  are smaller by an order of magnitude, while the amplitudes associated with  $O_8$  are highly suppressed. In table II, it is interesting to note that  $M_2^S$  adds constructively to  $M_7^S$ , *i.e.*,  $|M_2^S + M_7^S|^2 > |M_7^S|^2$ . On the contrary,  $M_2^P$  is destructive to  $M_7^P$ . Due to this cancelling effect, the inclusion of  $O_2$  contribution only enhances the total rate by 2% (This result is basically consistent with the estimation obtained in [13]). This result is not sensitive to the choice of  $\omega$ . We obtain the same enhancement for the total rate with  $\omega$  chosen to be 0.79 GeV and 0.80 GeV, respectively.

By fitting our prediction for the branching ratio  $\mathcal{B}(B \rightarrow K^*\gamma)$  to the CLEO data, we determine the  $B$  meson wave function,

$$\phi_B(x) = 0.740079 \sqrt{x(1-x)} \exp \left[ -\frac{1}{2} \left( \frac{xM_B}{0.795 \text{ GeV}} \right)^2 \right], \quad (38)$$

which possesses a sharp peak at the low momentum fraction  $x$ . We stress that, however, Eq. (38) is not conclusive because of the large allowed range of the shape parameter  $\omega$ . A more precise  $B$  meson wave function can be obtained by considering a global fit to the data of various decay modes, including  $B \rightarrow D^{(*)}\pi(\rho)$  [23]. Once the  $B$  meson wave function is fixed, we shall employ it in the evaluation of the nonleptonic charmless decays.

Finally, as mentioned in the Introduction, the authors of Ref. [14] found that the diagrams without hard-gluon exchanges dominate over Figs. 2(a) and 2(b) we have evaluated (only the operator  $O_7$  was considered in the calculation of the branching ratio  $\mathcal{B}(B \rightarrow K^*\gamma)$  in [14]): the latter contribute at most 23% to the branching ratio, or 12% to the decay amplitude. However, in that analysis,  $\alpha_s$  is set to 0.2, which is even smaller than  $\alpha_s(M_B) = 0.23$  evaluated at the  $B$  meson mass. We argue that such a small coupling constant is inappropriate, since the momentum flow involved in the decay process is most likely less than the  $b$  quark mass  $M_b$ , say, roughly  $1 \sim 2$  GeV, which corresponds to  $\alpha_s \approx 0.4$ . The  $K^*$  meson mass was neglected in [14], such that Fig. 2(a) does not contribute. In our analysis we did not make this approximation, and observed that the contribution from Fig. 2(a) is about  $M_{K^*}/M_B \approx 1/5$  of that from Fig. 2(b). Moreover, a flat  $B$  meson wave function corresponding to the shape parameter  $\omega \approx 1.3$  GeV was adopted in the computation of the higher-order contributions in [14], which is far beyond  $\omega \approx 0.4$  GeV specified in [22]. If a sharper  $B$  meson wave function is employed, these contributions will be enhanced at least by a factor of 3. Note that the leading-order contributions considered in [14] are less sensitive to the variation of  $\omega$  in the wave function. Adding up the above enhancements, the amplitude for  $O(\alpha_s)$ -corrections becomes approximately equal to the leading-order contribution. In this sense the analysis in [14] does not seem to be self-consistent. In our approach, the momentum of the spectator quark in the  $B$  meson is parametrized into the minus direction, while the momentum of the spectator quark in the  $K^*$  meson is parametrized in the plus direction. Under this parametrization, the diagrams without hard gluons do not contribute, because they violate the momentum conservation. That is, the diagrams we consider here are indeed leading.

## V. CONCLUSION

In this paper we have extended the PQCD three-scale factorization theorem to the penguin-induced radiative decay  $B \rightarrow K^* \gamma$ , which takes into account the Sudakov resummation for large logarithmic corrections to this process. We have included the non-spectator contribution from the current-current operator  $O_2$  besides the standard contribution given by magnetic-penguin operators  $O_7$  and  $O_8$ . It turns out that the contribution by  $O_2$  is negligible due to certain cancellations. The contributions from  $O_8$  and other operators in the effective Hamiltonian are also quite small. Finally, we have determined the  $B$  meson wave function from the best fit to the experimental data of  $\mathcal{B}(B \rightarrow K^* \gamma)$ , which will be employed to make predictions of other  $B$  meson decays.

## ACKNOWLEDGMENTS

We thank X.-G. He and W.-S. Hou for discussions. This work was supported in part by the National Science Council of R.O.C. under the Grant Nos. NSC-88-2112-M-006-013 and NSC-88-2112-M-009-002.

## REFERENCES

- [1] R. Ammar *et al.* (CLEO Collaboration), Phys. Rev. Lett. **71**, 674 (1993).
- [2] M. S. Alam *et al.* (CLEO Collaboration), Phys. Rev. Lett. **74**, 2885 (1995).
- [3] R. Ammar *et al.* (CLEO Collaboration), “*Radiative Penguin Decays of the B Meson*,” CONF 96-5, ICHEP-96 PA05-9 (1996).
- [4] S. Glenn *et al.* (CLEO collaboration), “*Improved Measurement of  $B(b \rightarrow s\gamma)$* ,” submitted to XXIX Int. Conf. on High Energy Physics, Vancouver, Canada, July 23-29, 1998.
- [5] B. Barate *et. al* (ALEPH), “*A Measurement of the Inclusive  $b \rightarrow s\gamma$  Branching Ratio*,” CERN-EP/98-044 (1998).
- [6] A. Falk, M. Luke and M. Savage, Phys. Rev. D **49**, 3367 (1994).
- [7] H-n. Li and H.L. Yu, Phys. Rev. Lett. **74**, 4388 (1995); Phys. Lett. B **353**, 301 (1995); Phys. Rev. D **53**, 2480 (1996).
- [8] H-n. Li, Phys. Rev. D **52**, 3958 (1995).
- [9] H-n. Li and H.L. Yu, Phys. Rev. D **53**, 4970 (1996).
- [10] C.H. Chang and H-n. Li, Phys. Rev. D **55**, 5577 (1997); T.W. Yeh and H-n. Li, Phys. Rev. D **56**, 1615 (1997).
- [11] V.L. Chernyak and A.R. Zhitnitsky, Phys. Rep. **112**, 173 (1984).
- [12] M. Benayoun and V.L. Chernyak, Nucl. Phys. **B 329**, 285 (1990).
- [13] J. Milana, Phys. Rev. D **53**, 1403 (1996).
- [14] C. Greub, H. Simma and D. Wyler, Nucl. Phys. **B 434**, 39 (1995).
- [15] For a review on earlier literatures, see G. Buchalla, A. J. Buras and M. E. Lautenbacher, Review of Modern Physics, **68**, 1125 (1996).
- [16] The signs of  $O_7$  and  $O_8$  are consistent with the covariant derivative  $D_\mu = \partial_\mu + igT^a A_\mu^a + ieQA_\mu$ , where  $A_\mu^a$  and  $A_\mu$  denote gluon and photon fields respectively.
- [17] Strictly speaking, the order of this diagram is  $eG_F(A_1\alpha_s \ln \frac{M_W}{\mu} + B_1\alpha_s + A_2\alpha_s^2 \ln^2 \frac{M_W}{\mu} + B_2\alpha_s^2 \ln \frac{M_W}{\mu} + \dots)$ , where coefficients  $A_i$  and  $B_i$  represent contributions from leading and next-to-leading logarithms. We simply count the order according to the first two terms in the series,  $A_1\alpha_s \ln \frac{M_W}{\mu}$  and  $B_1\alpha_s$ . Same rule of counting applies to diagrams in Fig. 1-3.
- [18] H.-Y. Cheng, C.-Y. Cheung, G.-L. Lin, Y.-C. Lin, T.-M. Yan and H.-L. Yu, Phys. Rev. D **51**, 1199 (1995).
- [19] J. Liu and Y.-P. Yao, Phys. Rev. D **42**, 1485 (1990).
- [20] This off-shell vertex was also calculated in Ref. [13], but the result was not presented explicitly.
- [21] F. Schlumpf, Report No. hep-ph/9211255; R. Akhoury, G. Sterman and Y.-P Yao, Phys. Rev. D **50**, 358 (1994).
- [22] M. Bauer and M. Wirbel, Z. Phys. C **42**, 671 (1989).
- [23] H-n. Li and B. Melic, in preparation.

## FIGURES

FIG. 1. Contributions to the  $B \rightarrow K^*\gamma$  decay from the current-current operator  $O_2$ . The diagram with a photon emitted from the other side of the charm-quark loop is not shown.

FIG. 2. Contributions to the  $B \rightarrow K^*\gamma$  decay from the magnetic-penguin operator  $O_7$ .

FIG. 3. Contributions to the  $B \rightarrow K^*\gamma$  decay from the chromo-magnetic-penguin operator  $O_8$ .

FIG. 4. Contributions to the  $B \rightarrow K^*\gamma$  decay from the strong-penguin operators  $O_3, O_4, \dots, O_6$ . The dark square denotes insertions of the operators  $O_3, O_4, \dots, O_6$ .

FIG. 5. Contributions to the  $B \rightarrow K^*\gamma$  decay from an  $O_2$ -insertion and a *bremsstrahlung* photon.

Table I. Hard subamplitudes obtained from Figs. 1-3. The quantities  $\tilde{A}_4$  and  $\tilde{A}_5$  are integrands of  $I_{11}$  and  $I_{20} - I_{10}$  respectively, where the general integral  $I_{ab}$  is defined in Eq. (10).

Diagram	$H^S$
$O_2$	$\frac{4}{3} \frac{(1-r)(1-r^2)x_K[(1-r^2+2rx_K+2x_B)\tilde{A}_4+(rx_K+3x_B)\tilde{A}_5]}{x_Kx_Bm_B^2+(\mathbf{k}_{KT}-\mathbf{k}_{BT})^2}$
$O_7(a)$	$\frac{2r(1-r^2)}{[x_Kx_Bm_B^2+(\mathbf{k}_{KT}-\mathbf{k}_{BT})^2][(x_B-r)m_B^2+k_{BT}^2]}$
$O_7(b)$	$\frac{2(1-r^2)[1+r+(1-2r)x_K]}{[x_Kx_Bm_B^2+(\mathbf{k}_{KT}-\mathbf{k}_{BT})^2](x_Km_B^2+k_{KT}^2)}$
$O_8(a)$	$-\frac{(1-r^2+x_B)(rx_K+x_B)}{3[x_Kx_Bm_B^2+(\mathbf{k}_{KT}-\mathbf{k}_{BT})^2][(1-r^2+x_B)m_B^2+k_{BT}^2]}$
$O_8(b)$	$-\frac{(2-3r)x_K-x_B+r(1-x_K)(rx_K-2rx_B+3x_B)}{3[x_Kx_Bm_B^2+(\mathbf{k}_{KT}-\mathbf{k}_{BT})^2][(x_K-1)m_B^2+k_{KT}^2]}$
$O_8(c)$	$-\frac{(1+r)(1-r^2)[(1+r)x_B-rx_K]}{3[(1-r^2)(x_B-x_K)m_B^2+(\mathbf{k}_{KT}-\mathbf{k}_{BT})^2][(1-r^2)x_Bm_B^2+k_{BT}^2]}$
$O_8(d)$	$\frac{(1-r^2)[(1-r^2)(2-x_K)+(1+3r)(2x_K-x_B)]+2r^2x_K(x_K-x_B)}{3[(1-r^2)(x_B-x_K)m_B^2+(\mathbf{k}_{KT}-\mathbf{k}_{BT})^2][(r^2-1)x_Km_B^2+k_{KT}^2]}$

---



---

Diagram

$H^P$

---

$$\begin{aligned}
O_2 & \frac{4}{3} \frac{(1-r^2)x_K[(1-r)(1-r^2) + 2r^2x_K + 2x_B]\tilde{A}_4 + (r(1+r)x_K + (3-rx_B))\tilde{A}_5]}{x_Kx_Bm_B^2 + (\mathbf{k}_{KT} - \mathbf{k}_{BT})^2} \\
O_7(a) & -\frac{2r(1-r^2)}{[x_Kx_Bm_B^2 + (\mathbf{k}_{KT} - \mathbf{k}_{BT})^2][(x_B - r)m_B^2 + k_{BT}^2]} \\
O_7(b) & -\frac{2(1-r^2)[1+r + (1-2r)x_K]}{[x_Kx_Bm_B^2 + (\mathbf{k}_{KT} - \mathbf{k}_{BT})^2](x_Km_B^2 + k_{KT}^2)} \\
O_8(a) & \frac{(1-r^2 + x_B)(rx_K + x_B)}{3[x_Kx_Bm_B^2 + (\mathbf{k}_{KT} - \mathbf{k}_{BT})^2][(1-r^2 + x_B)m_B^2 + k_{BT}^2]} \\
O_8(b) & \frac{(2-3r)x_K - x_B - r(1-x_K)(rx_K - 2rx_B + 3x_B)}{3[x_Kx_Bm_B^2 + (\mathbf{k}_{KT} - \mathbf{k}_{BT})^2][(x_K - 1)m_B^2 + k_{KT}^2]} \\
O_8(c) & \frac{(1-r)(1-r^2)[(1+r)x_B - rx_K]}{3[(1-r^2)(x_B - x_K)m_B^2 + (\mathbf{k}_{KT} - \mathbf{k}_{BT})^2][(1-r^2)x_Bm_B^2 + k_{BT}^2]} \\
O_8(d) & -\frac{(1-r^2)[(1-r^2)(2+x_K) - (1-3r)x_B] - 2r^2x_K(x_K - x_B)}{3[(1-r^2)(x_B - x_K)m_B^2 + (\mathbf{k}_{KT} - \mathbf{k}_{BT})^2][(r^2 - 1)x_Km_B^2 + k_{KT}^2]}
\end{aligned}$$


---

Table II. The amplitudes  $M_l^i$  in the unit of  $10^{-6} \text{ GeV}^{-2}$ .

$M_2^S/\Gamma_0$	$M_7^S/\Gamma_0$	$M_8^S/\Gamma_0$
$-2.46 - 14.17i$	$-140.14 - 143.31i$	$-0.58 + 1.10i$
$M_2^P/\Gamma_0$	$M_7^P/\Gamma_0$	$M_8^P/\Gamma_0$
$-1.21 - 11.05i$	$140.14 + 143.31i$	$0.54 - 1.33i$

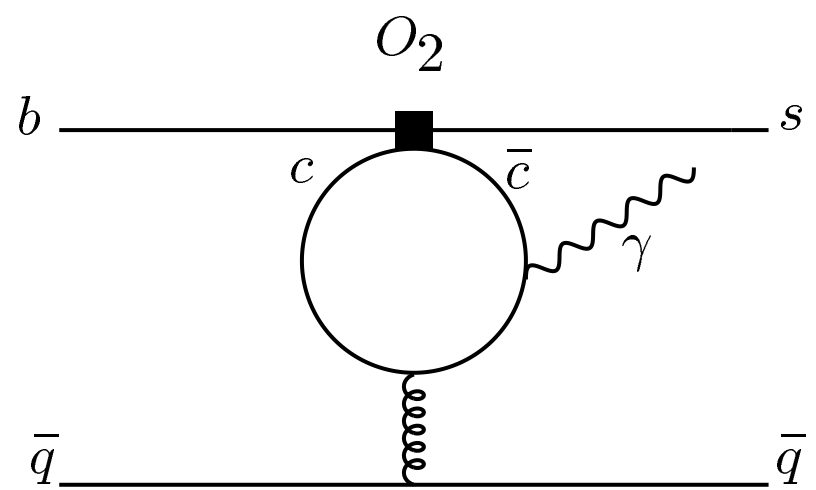
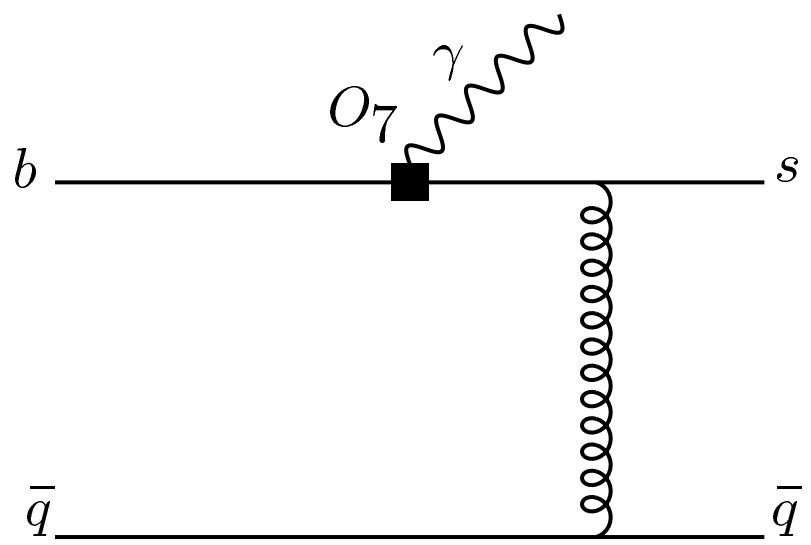
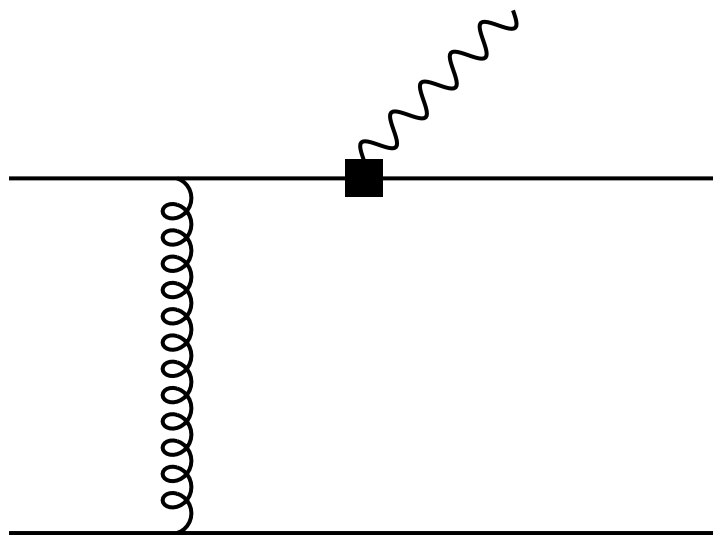


Fig. 1

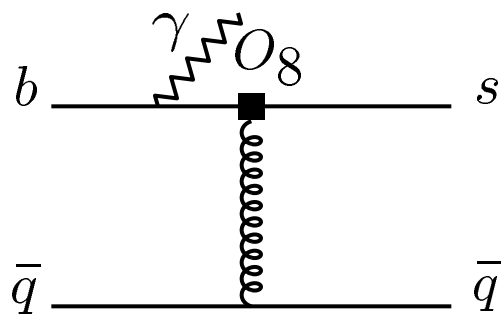


(a)

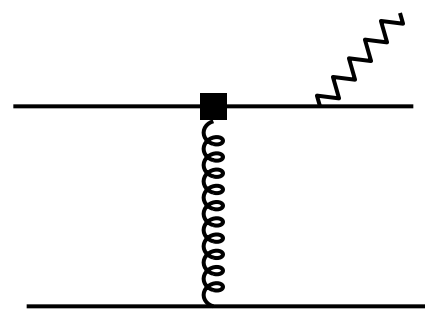


(b)

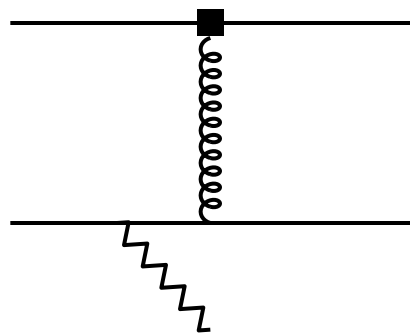
Fig. 2



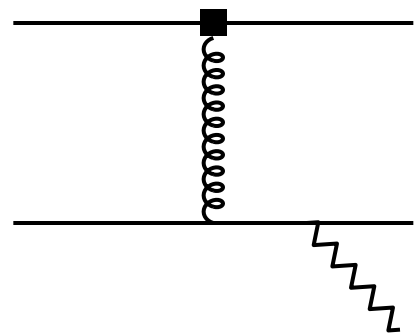
(a)



(b)



(c)



(d)

Fig. 3

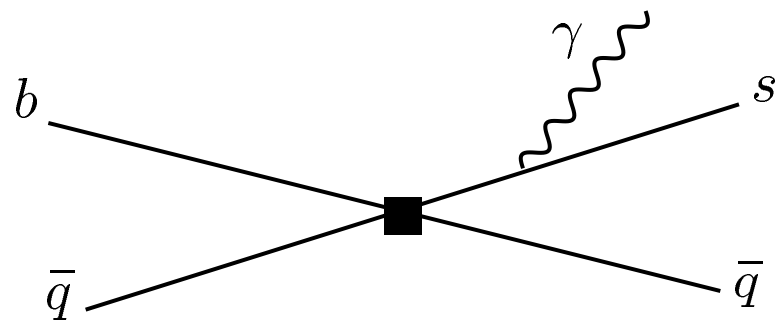


Fig. 4

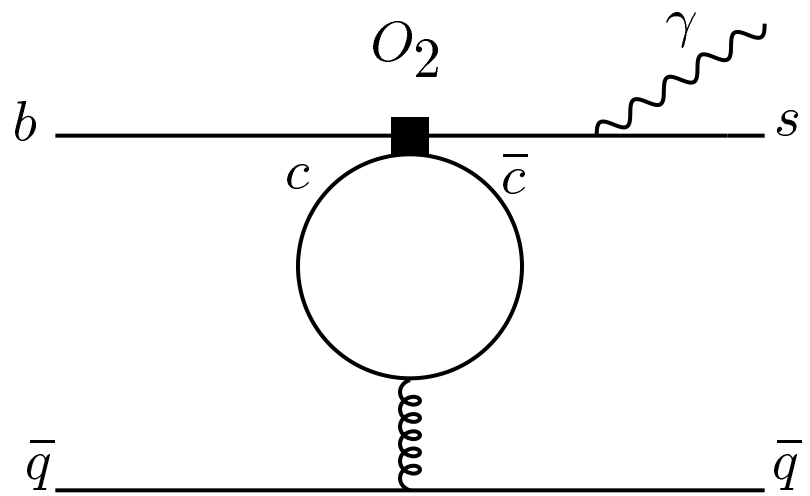


Fig. 5